IEEE Photonics Journal
An IEEE Photonics Society Publication

Open Access

Vector Effects of Dissipative Soliton in All-Fiber MOPA System

(Invited Paper)

Volume 11, Number 6, December 2019

Xiang-Yue Li
Shi-Lin Liu
Meng Liu
Ai-Ping Luo
Zhi-Chao Luo, ***Member, IEEE***
Wen-Cheng Xu

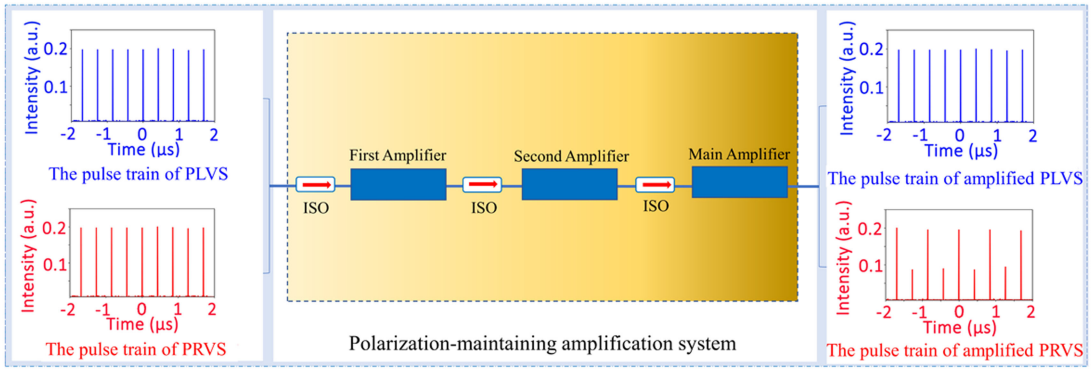

DOI: 10.1109/JPHOT.2019.2941563

Vector Effects of Dissipative Soliton in All-Fiber MOPA System

(Invited Paper)

Xiang-Yue Li, Shi-Lin Liu, Meng Liu, Ai-Ping Luo, Zhi-Chao Luo, *Member, IEEE*, and Wen-Cheng Xu

Guangdong Provincial Key Laboratory of Nanophotonic Functional Materials and Devices & Guangzhou Key Laboratory for Special Fiber Photonic Devices and Applications, South China Normal University, Guangzhou 510006, China

DOI:10.1109/JPHOT.2019.2941563

Manuscript received July 31, 2019; revised September 9, 2019; accepted September 11, 2019. Date of publication September 18, 2019; date of current version October 28, 2019. This work was supported in part by National Natural Science Foundation of China (NSFC) (11874018, 11474108, 61875058, and 61805084), in part by Guangdong Natural Science Funds for Distinguished Young Scholar (2014A030306019), in part by Guangdong Key R&D Program (2018B090904003), in part by Science and Technology Project of Guangdong (2016B090925004), in part by Foundation for Young Talents in Higher Education of Guangdong, China under Grant 2017KQNCX051, in part by Scientific Research Foundation of Young Teacher of South China Normal University, China under Grant 17KJ09, in part by Open Fund of the Guangdong Provincial Key Laboratory of Fiber Laser Materials and Applied Techniques (South China University of Technology). Corresponding authors: Zhi-Chao Luo; Wen-Cheng Xu (e-mail: zcluo@scnu.edu.cn; xuwch@scnu.edu.cn).

Abstract: The performance of seed laser source will have a great impact on the output pulse quality of the master oscillator power amplifier (MOPA) system. Here, we report the influence of the soliton vector features on the pulse uniformity in an all-fiber MOPA configuration. We demonstrated that, although the intensity of the dissipative soliton seed source is uniform, the intensity of the output pulse train from the MOPA will show fluctuations if the soliton polarization state is not locked, i.e., polarization-rotating vector soliton. It is found that the appearance of non-uniform pulse intensity is caused by the combination of the polarization instability and the polarization dependent gain in the polarization maintaining fiber amplifier. The obtained results indicate that the polarization evolution of seed pulsed source is critical to generation of stable pulse train from the MOPA, and also might be useful to the communities dealing with solitons and high-power pulsed fiber lasers.

Index Terms: Dissipative vector solitons, fiber lasers, MOPA, high-energy pulses.

1. Introduction

High power, ultrashort pulse fiber laser technologies have attracted much attention owing to their wide applications in scientific and industrial fields such as ultrafast optics exploration, biomedicine, and laser micromachining [1]–[4]. The passive mode-locking is regarded as an efficient method to generate the ultrashort pulse from fiber lasers [5]–[7]. However, owing to the nonlinear effects induced pulse instability [8]–[9], the direct output of high-power ultrashort pulse from a mode-locked fiber oscillator remains a challenging task. Although the dissipative soliton (DS) formation in normal dispersion fiber laser was proposed to enhance the pulse stability and energy [10]–[11], the output pulse energy is still limited to be the order of nJ, which is insufficient for some practical applications. To boost the output power of ultrashort pulse, the fiber master oscillator power amplifier (MOPA)

system can be employed, which has been demonstrated to be one of the efficient methods to realize power and energy scaling [12]–[16]. Generally, the polarization-maintaining (PM) fiber amplification system is used to improve environmental stability. Up to now, the output energy of ultrashort pulse with MOPA system is easy to reach the micro-joule levels [17], [18], which greatly extends the range of application fields.

Apart from the power scaling ability, the intensity uniformity of the output pulse train from a MOPA system is also important to the applications. In fact, it is found that the polarization-dependent gain is a well-known effect and should be considered in the fiber amplifier [19]–[21]. The polarization related gain characteristics will make the signal gains of two orthogonal polarization directions different from each other. In this sense, any polarization instabilities of seed pulse signal will lead to the intensity fluctuations after the MOPA. On the other hand, the passively mode locked ultrafast fiber laser is one of the most frequently used seed pulse signals for MOPA. In general, for the purpose of low-cost and reliable operation, ultrafast fiber laser is constructed with non-PM fiber and real saturable absorber. It has been demonstrated that the ultrashort pulse, which is also regarded as optical soliton, would exhibit fruitful polarization dynamics in the ultrafast fiber lasers as the result of the single mode fiber (SMF) supporting the two orthogonal polarization modes. So far, various vector soliton dynamics could be observed in passively mode locked fiber lasers [22]–[34], such as polarization-locked vector solitons (PLVSs) [22]–[24], [29], [30] and polarization-rotating vector solitons (PRVSs) [31]–[33]. Being different from the PLVS, the PRVS features that the pulse intensities along the two polarization components varied periodically with the cavity roundtrip time. In addition, the operation regimes between PLVS and PRVS in the fiber laser could be transited if the pump power or birefringence variations are introduced. Therefore, the appearance of PRVS could be deemed as a potential polarization instability in the mode locked lasers. Considering the polarization characteristics of vector solitons and the polarization-dependent gain in fiber amplifier, it is interesting to identify the influence of vector features of dissipative soliton on the performance of MOPA system.

In this work, we investigated the vector effects of dissipative soliton in a PM-MOPA system. Both the PLVSs and PRVSs could be obtained in the mode locked fiber oscillator by adjusting the polarization controller (PC) at a fixed pump power. Then we injected the PLVS and PRVS as seed pulse signal into the fiber amplifiers, respectively. It was found that for the case of PRVS the intensity of the output pulse from MOPA would show periodical fluctuations, where the modulation period of the pulse intensity corresponds to the soliton polarization rotation period. However, for PLVS as the seed signal, the pulse intensity after the fiber amplifiers is still uniform. We attributed this phenomenon to the polarization dependent gain of active fiber and the unlocked polarization state of the dissipative soliton. The average power of the pulse after the PM-MOPA system reaches 3.96 W at the pump power of 17 W, corresponding to $\sim$1.67 μJ of pulse energy. The results demonstrated that the vector soliton characteristics of the seed source need to be considered in the MOPA system, which is beneficial for achieving the stable pulse train from the MOPA.

2. Experimental Setup

Fig. 1 shows the experimental setup of the proposed all-fiber MOPA system. A passively mode locked fiber laser based on a saturable absorber (BATOP SA-1064-26-37ps) is used as the seed source, as shown in Fig. 1(a). A 1-m long highly Yb-doped fiber (YDF) is served as the gain medium. The cavity birefringence and the polarization state of the propagation light are adjusted by the PC. A polarization-independent isolator (PI-ISO) ensures the unidirectional operation, and the band-pass filter with a 3-dB spectral bandwidth of $\sim$5 nm is utilized for wavelength selection and stabilizing the mode locking operation [35]. As there are no polarization discrimination devices in the laser cavity, the polarization state of the mode locked soliton can evolve freely to form different types of vector solitons [31].

The output of the oscillator was coupled into the amplifier stage via a PM isolator. The PM isolators between each stage are used to prevent the backscattering light from damaging the cavity in the previous stage. It should be noted that the injected pulse train has no polarization dependent loss in

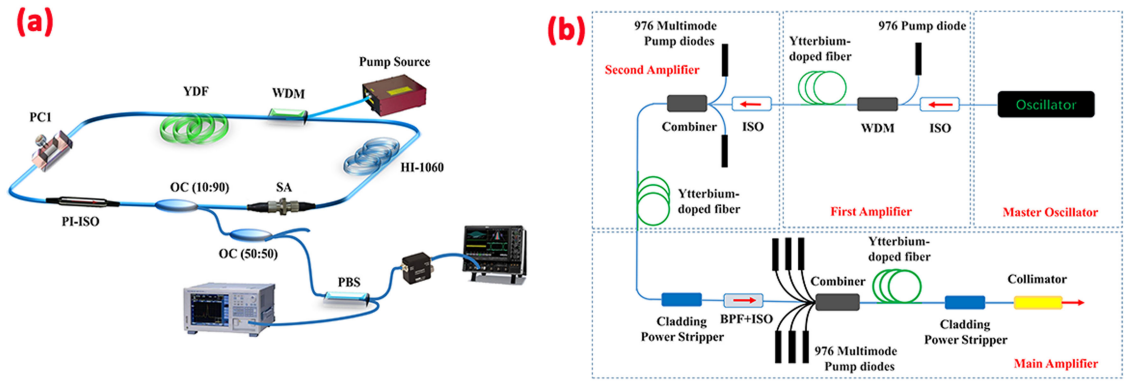

Fig. 1. Schematics of all-fiber MOPA. (a) the seed laser, WDM: wavelength division multiplexer; PC: polarization controller; PI-ISO: polarization dependent isolator; YDF: Yb-doped fiber; OC: optical coupler; BPF: band pass filter; SMF: HI-1060; SA: saturable absorber; (b) the cascaded amplifiers, CPS: cladding power stripper; BPF + ISO: band pass filter isolator.

the dual-axis operation PM isolators. Two preamplifiers are used to achieve sufficient power to seed the final-stage main amplifier. For the first amplifier, the gain medium is the 1-m PM highly Yb-doped fiber (YDF) with a core/cladding diameter of 6/125 μm, which is core-pumped by a single-mode (SM) 976 nm laser diode through wavelength division multiplexer (WDM). For second preamplifier, a $(2 + 1) \times 1$ signal/pump combiner is utilized for matching the 10/125 μm large-mode-area (LMA) double-clad YDF (Nufern PLMA-YDF-10/125-HI-8) which was pumped by two multimode double-clad 976 nm LDs. The unabsorbed pump light is dumped by a cladding power stripper (CPS). The PM bandpass filter isolator here is adopted to prevent the backward reflections and to suppress the amplified spontaneous emission (ASE) at short wavelength. The main amplifier consists of a $\sim$2.8 m highly double-clad YDF (Liekki Yb 1200-30/250 DC-PM) with a core/cladding diameter of 30/250 μm. The length of YDF is optimized to control the fiber nonlinearity. This gain fiber is clad-pumped by two multimode 976 LDs with a maximum pump power of 28 W. The single-mode operation was obtained by coiling the gain fiber to a diameter of 12 cm to introduce additional bend-induced losses for the higher-order modes. The output laser is monitored by an optical spectrum analyzer (OSA, Yokogawa AQ6317C) and a high-speed real-time oscilloscope (Tektronix DSA-70804, 8 GHz) with a photodetector (Newport 818-BB-35F, 12.5 GHz). In order to observe the vector nature of multi-soliton patterns, a PC and a fiber-based polarization beam splitter (PBS) are used to resolve the dynamics of the two polarization components. The pulse duration was measured by a commercial autocorrelator (FR-103WS).

3. Results

Owing to the existence of saturable absorber in the laser cavity, the fiber laser can easily turn into the mode locked state if the pump power level is above the lasing threshold. In the experiment, the mode locked threshold is about 48 mW. The fiber laser could operate either in single pulse or in the multi-pulse regimes, which is dependent on the pump power level. For enabling the fiber laser to operate in the single pulse state, we adjusted the pump power to be 51 mW and fixed it in the following experiment. Fig. 2(a) shows the typical mode locked spectrum of the fiber laser. The appearance of the steep spectral edges indicates that the fiber laser was operating in dissipative soliton regime with normal dispersion. The central wavelength and the 3-dB spectral bandwidth are 1069.75 nm and $\sim$2.3 nm, respectively. The mode locked pulse train is plotted in Fig. 2(b). Here, the pulse separation is 423 ns, corresponding to the fundamental repetition of 2.364 MHz. The autocorrelation trace shows that the pulse duration is $\sim$215 ps, which gives a time-bandwidth product about 66.4. Thus, the mode locked pulse is highly chirped.

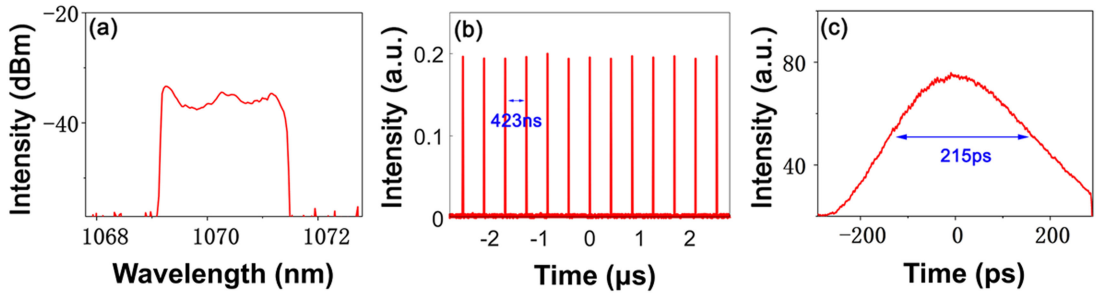

Fig. 2. Typical performance of the mode locked fiber oscillator. (a) Optical spectrum; (b) mode-locked pulse train; (c) autocorrelation trace.

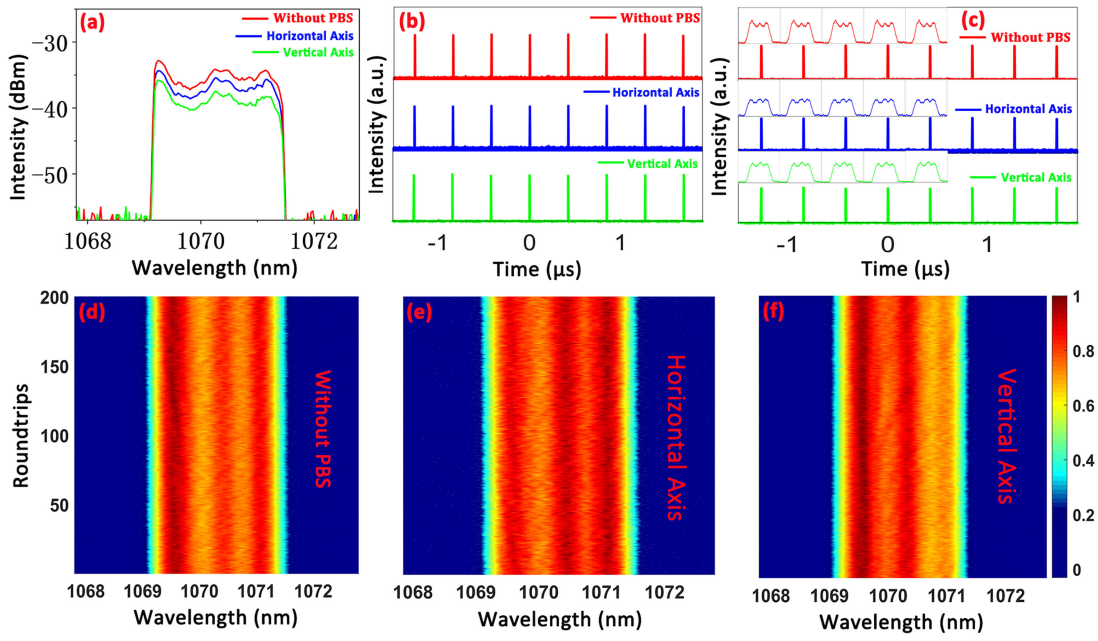

Fig. 3. Polarization-resolved measurements of PLVS regime. (a) Spectra; (b) pulse trains; (c) pulse trains after DFT process; and (d)–(f) shot-to-shot spectra of 200 successive roundtrips.

As indicated above, no polarization discrimination devices were in the laser cavity. Therefore, the fiber laser could be used to investigate the dynamics of vector solitons. Fig. 3 shows the polarization resolved measurements of the vector soliton corresponding to the state of Fig. 2. From the spectral domain, it can be seen that two polarization components show the similar spectral profiles, as depicted in Fig. 2(a). Meanwhile, the total pulse train as well as those of two polarization components present the uniform intensity. The spectral and temporal features of the soliton suggest that the fiber laser delivers the PLVS in this case. In order to investigate the spectral characteristics of the PLVS, the real-time spectroscopy technology, namely dispersion Fourier transformation (DFT) [36]–[38] was employed to capture the real-time spectral dynamics. Fig. 3(c) provides the shot-to-shot spectra of the total pulse train and the two polarization components after the PBS, where the uniform spectral profiles can be seen for the PLVS. To further demonstrate the stability of the mode locked oscillator, we provided the shot-to-shot spectra of 200 successive roundtrips in Figs. 3(d) to 3(f). Again, the profiles of each shot-to-shot spectrum are nearly indistinguishable from one another. These results demonstrated that no polarization instability was detected in the mode locked fiber oscillator. Thus, the mode locked laser could be employed as the stable seed source in MOPA system.

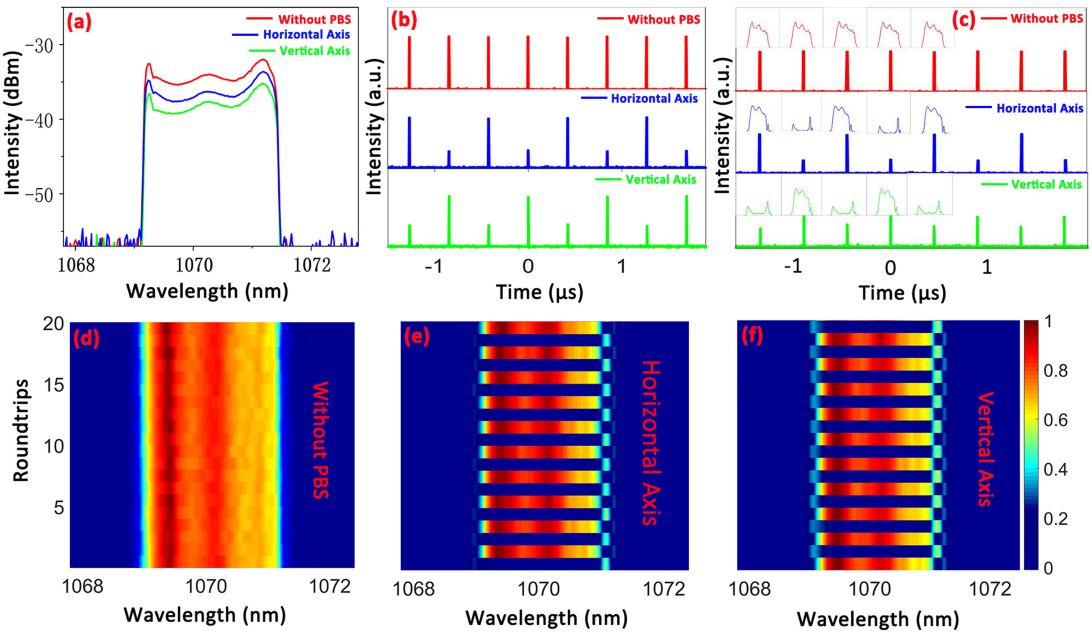

Fig. 4. Polarization-resolved measurements of PRVS regime. (a) Optical spectra; (b) pulse trains; (c) pulse trains after a DFT process; and (d)–(f) shot-to-shot spectra of 20 successive roundtrips.

By carefully adjusting the orientation of the PC, the operation regime of PLVS can be converted into the PRVS in the fiber laser. The measured characteristics of the PRVS were plotted in Fig. 4. The OSA-recorded spectra with and without the PBS are presented in Fig. 4(a), where the spectral profiles are similar to each other. The OSA-measured spectral features of the PRVS could not be evidently distinguished from those of the PLVS. However, being different from the case of PLVS, the polarization state of the soliton is rotating periodically at a fixed output point of the fiber laser. Therefore, one of the typical features of PRVS is that the intensities of the two polarization components will present periodic modulation after passing the PBS, as shown in Fig. 4(b). Because the intensity of the pulses along the two-polarization direction varied periodically, the real-time spectrum should be changed with the cavity roundtrip time. Then the DFT was employed again to measure the real-time spectral dynamics of PRVS. In Fig. 4(c), it is clearly seen that the peak intensity and the profile of the real-time mode locked spectrum along the two orthogonal polarization components altered periodically, which is similar to those we have previously reported [39]. For better clarity, we have also provided that real-time spectral dynamics by DFT for 20 cavity roundtrips in Figs. 4(d)-4(f). As the polarization unresolved spectrum and pulse intensity of PRVS before passing the PBS are stable on the OSA and oscilloscope, respectively, the instability of the two polarization components is generally ignored as the seed laser source in MOPA system. However, considering the polarization-dependent gain in YDF, it is expected that the polarization instability of the PRVS will induce the output instability of the MOPA system.

In order to investigate the influence of the vector nature of dissipative soliton on the MOPA system, we injected both the PLVS and PRVS as the seed sources into the fiber amplifiers, respectively. After pulse amplification, both the PLVS and PRVS could be boosted to around 3.5 W at the pump power of ∼17 W. Here, it should be noted that the stability of the output pulse could be limited by appearance of Raman effect with higher pump power level of the MOPA system. Fig. 5(a) and 5(b) shows the pulse train and the spectrum of the amplified PLVS. Because the polarization of the mode-locked seed pulse is locked, the intensity of the output pulse train is uniform despite of the polarization-dependent gain of YDF. The amplified spectrum is similar to that of the seed pulse. However, when the PRVS was used as the input for the MOPA system, the evident intensity modulation on the pulse train could be observed. The spectral and temporal features of PRVS after

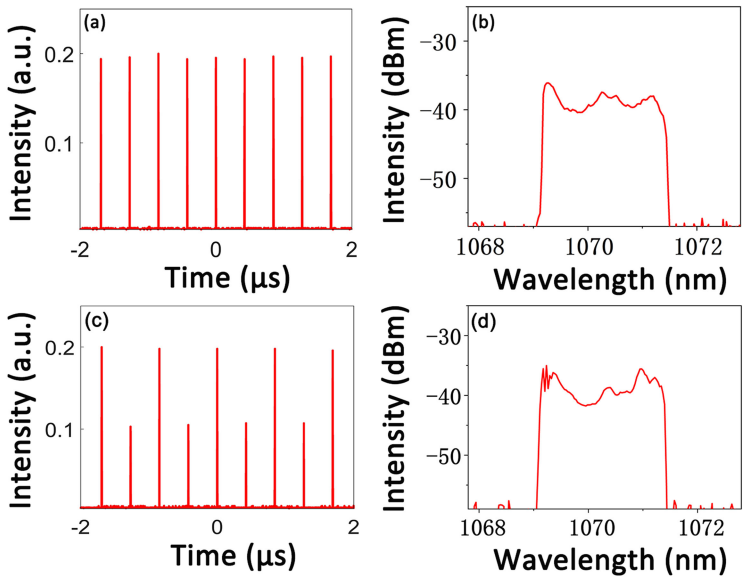

Fig. 5. Amplified pulse trains and spectra of PLVS and PRVS. (a) Oscilloscope traces of PLVS; (b) spectrum of amplified PLVS; (c) oscilloscope traces of PRVS; (d) amplified spectrum of PRVS.

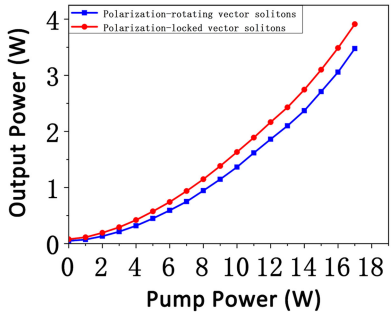

Fig. 6. Output power of the amplified PLVS and PRVS versus pump power.

amplification is presented in Figs. 5(c) and 5(d). Here, the pulse train shows a modulation period of two cavity roundtrips which is the same as the polarization rotation period. Therefore, it further confirms that the intensity modulation was caused by the polarization instability of the PRVS. Note that there is a slight spectral modulation on the left edge of the corresponding spectrum, which might result from the intensity fluctuation of the amplified pulse and the nonlinear effect, as shown in Fig. 5(d). In addition, the vector nature of PRVS after amplification was also checked by using a PBS. It is found that the PRVS still maintains the polarization rotation characteristic.

To further exhibit the performance of the MOPA system, we have provided the average output power of the amplified PLVS and PRVS versus the pump power in Fig. 6. Here, the average output power increases with higher pump power. Note that the input powers of PLVS and PRVS for MOPA are adjusted to be the same as each other, which are $\sim$880 μw. The maximum output power can reach to about 3.9 W for the case of PLVS, which is corresponding to the single pulse energy of 1.65 μJ. However, at a lower pump power, the slope efficiency of the MOPA system is lower than that of the higher pump power level. We think that this phenomenon is related to the reabsorption of the YDF owing to the unoptimized length of the YDF. From Fig. 6, it should be noted that the average output power of PLVS is a little higher than that of PRVS for the same MOPA parameters, which could be attributed to the non-uniform power amplification of the PRVS.

In general, for MOPA system the quality of the output pulse is important to the practical applications. Thus, the output pulse with intensity modulation will degrade the laser performance. As mentioned above, the total intensities of PRVS and PLVS are detected to be uniform from the oscilloscope, which are generally regarded as the stable seed source. However, in our experiments, it has been demonstrated that the vector nature of the seed laser pulse greatly influences the intensity uniformity of the output pulse. That is, in order to improve the stability of the MOPA system, the polarization of the seed pulse needs to be locked. On the other hand, we only observed the polarization instability induced non-uniform intensity of pulse train from MOPA system. And there are few reports on the polarization dependent gain of the PM YDF. Therefore, the polarization dependent gain feature also needs to be further investigated, which will be beneficial for generating the stable pulse of MOPA system if a non-PM mode locked oscillator is employed.

4. Conclusions

In summary, we have investigated the influence of the mode locked soliton polarization on the pulse stability in a MOPA system. It was found that the output pulse shows periodic modulation after the PM amplification when the PRVS was employed as the seed pulse. However, for the case of PLVS, the output pulse after amplification maintains uniform intensity. The polarization instability of PRVS and the polarization dependent gain of PM YDF are demonstrated to be responsible for the appearance of the intensity modulation of output pulse train from MOPA system. Our findings will enhance the understanding of the dissipative vector solitons in MOPA system, which might be attractive to the communities dealing with high power fiber lasers and nonlinear optics.

References

[1] K. F. MacDonald, Z. L. Sámson, M. I. Stockman, and N. I. Zheludev, "Ultrafast active plasmonics," *Nature Photon.*, vol. 3, no. 1, pp. 55–58, Dec. 2009.
[2] X. Liu, D. Du, and G. Mourou, "Laser ablation and micromachining with ultrashort laser pulses," *IEEE J. Sel. Topics Quantum Electron.*, vol. 33, no. 10, pp. 1706–1716, Oct. 1997.
[3] C. Dunsby, P. M. P. Lanigan, J. McGinty, D. S. Elson, and P. M. W. French, "An electronically tunable ultrafast laser source applied to fluorescence imaging and fluorescence lifetime imaging microscopy," *J. Phys. D*, vol. 37, pp. 3296–3303, Nov. 2004.
[4] C. B. Schaffer, A. Brodeur, J. F. Garcia, and E. Mazur, "Micromachining bulk glass by use of femtosecond laser pulses with nanojoule energy," *Opt. Lett.*, vol. 26, no. 2, pp. 93–95, Jan. 2001.
[5] K. Tamura, E. P. Ippen, H. A. Haus, and L. E. Nelson, "77-fs pulse generation from a stretched-pulse mode-locked all-fiber ring laser," *Opt. Lett.*, vol. 18, no. 13, pp. 1080–1083, Jul. 1993.
[6] M. Hofer, M. H. Ober, F. Haberl, and M. E. Fermann, "Characterization of ultrashort pulse formation in passively mode-locked fiber lasers," *IEEE J. Quantum Electron.*, vol. 28, no. 3, pp. 720–728, Mar. 1992.
[7] X. Zhu *et al.*, "TiS 2-based saturable absorber for ultrafast fiber lasers," *Photon. Res.*, vol. 6, no. 10, pp. C44–C48, Oct. 2018.
[8] R. H. Stolen and A. M. Johnson, "Optical wave breaking of pulses in nonlinear optical fibers," *Opt. Lett.*, vol. 10, no. 9, pp. 457–459, Sep. 1985.
[9] D. Anderson, M. Desaix, M. Lisak, and M. L. Quiroga, "Wave breaking in nonlinear-optical fibers," *J. Opt. Soc. Amer. B.*, vol. 9, no. 8, pp. 1358–1361, Aug. 1992.
[10] F. O. Ilday, J. R. Buckley, W. G. Clark, and F. W. Wise, "Self-similar evolution of parabolic pulses in a laser," *Phys. Rev. Lett.*, vol. 92, no. 21, May 2004, Art. no. 213902.
[11] A. Chong, W. H. Renninger, and F. W. Wise, "All-normal-dispersion femtosecond fiber laser with pulse energy above 20 nJ," *Opt. Lett.*, vol. 32, no. 16, pp. 2408–2410, Aug. 2007.
[12] G. A. Ball, C. E. Holton, G. Ahull-Allen, and W. W. Morey, "60 mW 1.5/spl mu/m single-frequency low-noise fiber laser MOPA," *IEEE Photon. Technol. Lett.*, vol. 6, no. 2, pp. 192–194, Feb. 1994.
[13] J. Liu, Q. Wang, and P. Wang, "High average power picosecond pulse generation from a thulium-doped all-fiber MOPA system," *Opt. Exp.*, vol. 38, no. 20, pp. 4150–4153, Oct. 2013.
[14] X. Wang, P. Zhou, X. L. Wang, H. Xiao, and L. Si, "102 W monolithic single frequency Tm-doped fiber MOPA," *Opt. Exp.*, vol. 21, no. 26, pp. 2408–2410, Dec. 2013.
[15] J. Liu, H. Shi, K. Liu, Y. Hou, and P. Wang, "210 W single-frequency, single-polarization, thulium-doped all-fiber MOPA," *Opt. Exp.*, vol. 22, no. 21, pp. 13572–13578, May 2014.
[16] T. H. Loftus *et al.*, "522 W average power spectrally beam-combined fiber laser with near-diffraction-limited beam quality," *Opt. Lett.*, vol. 32, no. 4, pp. 349–351, Feb. 2007.
[17] C. Wandt *et al.*, "High-energy, diode-pumped, nanosecond Yb:YAG MOPA system," *Opt. Lett.*, vol. 33, no. 10, pp. 1111–1113, May 2008.

[18] A. Dergachev, D. Armstrong, A. Smith, T. Drake, and M. Dubois, "3.4-μm ZGP RISTRA nanosecond optical parametric oscillator pumped by a 2.05-μm Ho:YLF MOPA system," *Opt. Exp.*, vol. 15, no. 22, pp. 14404–14413, Oct. 2007.
[19] V. J. Mazurczyk and J. L. Zyskind, "Polarization dependent gain in erbium-doped fiber amplifiers," *IEEE Photon. Technol. Lett.*, vol. 6, no. 5, pp. 616–618, May 1994.
[20] P. Wysocki and V. Masurzyk, "Polarization dependent gain in erbium-doped fiber amplifiers: Computer model and approximate formulas," *J. Lightw. Technol.*, vol. 14, no. 4, pp. 572–584, Apr. 1996.
[21] P. Weels and C. Fallnich, "Polarization dependent gain in neodymium and ytterbium doped fiber amplifiers," *Opt. Exp.*, vol. 11, no. 6, pp. 530–534, Mar. 2003.
[22] S. T. Cundiff, B. C. Collings, N. N. Akhmediev, J. M. Soto-Crespo, K. Bergman, and W. H. Knox, "Observation of polarization-locked vector solitons in an optical fiber," *Phys. Rev. Lett.*, vol. 82, no. 20, pp. 3988–3991, May 1999.
[23] S. T. Cundiff, B. C. Collings, and W. H. Knox, "Polarization locking in an isotropic, mode-locked soliton Er/Yb fiber laser," *Opt. Exp.*, vol. 1, no. 1, pp. 12–20, Jul. 1997.
[24] D. Y. Tang, H. Zhang, L. M. Zhao, and X. Wu, "Observation of high-order polarization-locked vector solitons in a fiber laser," *Phys. Rev. Lett.*, vol. 101, no. 15, Oct. 2008, Art. no. 153904.
[25] Z. Wu, D. Liu, S. Fu, L. Li, M. Tang, and L. Zhao, "Scalar-vector soliton fiber laser mode-locked by nonlinear polarization rotation," *Opt. Exp.*, vol. 24, pp. 18764–18771, Aug. 2016.
[26] L. M. Zhao, D. Y. Tang, H. Zhang, X. Wu, and N. Xiang, "Soliton trapping in fiber lasers," *Opt. Exp.*, vol. 16, no. 13, pp. 9528–9533, Jun. 2008.
[27] H. Zhang, D. Y. Tang, L. M. Zhao, X. Wu, and H. Y. Tam, "Dissipative vector solitons in a dispersion-managed cavity fiber laser with net positive cavity dispersion," *Opt. Exp.*, vol. 17, no. 2, pp. 455–460, Jan. 2009.
[28] D. Mao, X. Liu, and H. Lu, "Observation of pulse trapping in a near-zero dispersion regime," *Opt. Lett.*, vol. 37, no. 13, pp. 2619–2621, Jul. 2012.
[29] C. Mou, S. Sergeyev, A. Rozhin, and S. Turistyn, "All-fiber polarization locked vector soliton laser using carbon nanotubes," *Opt. Lett.*, vol. 36, no. 19, pp. 3831–3833, Oct. 2011.
[30] S. Sergeyev, C. Mou, A. Rozhin, and S. K. Turitsyn, "Vector solitons with locked and precessing states of polarization," *Opt. Exp.*, vol. 20, no. 24, pp. 27434–27440, Nov. 2012.
[31] L. M. Zhao, D. Y. Tang, X. Wu, H. Zhang, and H. Y. Tam, "Coexistence of polarization-locked and polarization-rotating vector solitons in a fiber laser with SESAM," *Opt. Lett.*, vol. 34, no. 20, pp. 3059–3061, 2009.
[32] Q. Y. Ning *et al.*, "Vector nature of multi-soliton patterns in a passively mode-locked figure-eight fiber laser," *Opt. Exp.*, vol. 22, no. 10, pp. 11900–11911, May 2014.
[33] X. Z. Yuan *et al.*, "Experimental observation of vector solitons in a highly birefringent cavity of ytterbium-doped fiber laser," *Opt. Exp.*, vol. 21, no. 20, pp. 23886–23892, Sep. 2013.
[34] X. Zhao, T. Li, Y. Liu, Q. Li, and Z. Zheng, "Polarization-multiplexed, dual-comb all-fiber mode-locked laser," *Photon. Res.*, vol. 6, no. 9, pp. 853–857, Sep. 2018.
[35] B. G. Bale, J. N. Kutz, A. Chong, W. H. Renninger, and F. W. Wise, "Spectral filtering for high-energy mode-locking in normal dispersion fiber lasers," *J. Opt. Soc. Amer. B.*, vol. 25, no. 10, pp. 1763–1770, Oct. 2008.
[36] T. Jannson, "Real-time Fourier transformation in dispersive optical fibers," *Opt. Lett.*, vol. 8, no. 4, pp. 232–234, Apr. 1983.
[37] Y. C. Tong, L. Y. Chan, and H. K. Tsang, "Fiber dispersion or pulse spectrum measurement using a sampling oscilloscope," *Electron. Lett.*, vol. 33, no. 11, pp. 983–985, May 1997.
[38] K. Goda and B. Jalali, "Dispersive Fourier transformation for fast continuous single-shot measurements," *Nature Photon.*, vol. 7, pp. 102–112, Feb. 2013.
[39] M. Liu, A.-P. Luo, Z.-C. Luo, and W.-C. Xu, "Dynamic trapping of a polarization rotation vector soliton in a fiber laser," *Opt. Lett.*, vol. 42, no. 2, pp. 330–333, Jan. 2017.